Petroleum 1 (2015) 68–74

Contents lists available at ScienceDirect

Petroleum

journal homepage: www.keaipublishing.com/en/journals/petlm

Original article

Numerical analysis of non-Newtonian rheology effect on hydrocyclone flow field

Lin Yang [a], Jia-Lin Tian [a, b, *], Zhi Yang [a], You Li [a], Chuan-Hong Fu [a], Yong-Hao Zhu [a], Xiao-Lin Pang [a]

[a] School of Mechanical Engineering, Southwest Petroleum University, Chengdu 610500, China
[b] School of Mechanical Engineering, Southwest Jiaotong University, Chengdu 610031, China

ARTICLE INFO

Article history:
Received 28 January 2015
Received in revised form
27 April 2015
Accepted 4 May 2015

Keywords:
Non-Newtonian rheology
Cyclone separation
Key parameters
Turbulent drag reduction
FLUENT

ABSTRACT

In view of the limitations of the existing Newton fluid effects on the vortex flow mechanism study, numerical analysis of non Newton fluid effects was presented. Using Reynolds stress turbulence model (RSM) and mixed multiphase flow model (Mixture) of FLUENT (fluid calculation software) and combined with the constitutive equation of apparent viscosity of non-Newtonian fluid, the typical non-Newtonian fluid (drilling fluid, polymer flooding sewage and crude oil as medium) and Newton flow field (water as medium) were compared by quantitative analysis. Based on the research results of water, the effects of non-Newtonian rheology on the key parameters including the combined vortex motion index n and tangential velocity were analyzed. The study shows that: non-Newtonian rheology has a great effect on tangential velocity and n value, and tangential velocity decreases with non-Newtonian increasing. The three kinds of n values (constant segment) are: 0.564(water), 0.769(polymer flooding sewage), 0.708(drilling fluid) and their variation amplitudes are larger than Newtonian fluid. The same time, non-Newtonian rheology will lead to the phenomenon of turbulent drag reduction in the vortex flow field. Compared with the existing formula calculation results shown, the calculation result of non-Newtonian rheology is most consistent with the simulation result, and the original theory has large deviations. The study provides reference for theory research of non-Newtonian cyclone separation flow field.

1. Introduction

Hydrocyclone is widely used because of many advantages, which has a broad application prospect [1] in oil industry, such as mud purification, oil-water separation, heavy oil and sewage treatment etc. Although the cyclone structure is very simple, its internal flow field is quite complex, which is a strong rotational flow field with high turbulence. Related studies [2] have shown that the combination vortex motion in the hydrocyclone is formed under the specific parameters condition. Because the value of movement index n directly determines tangential velocity distribution of flow field and the value of tangential velocity directly determines the cyclone's almost all key parameters (separation size, production capacity and separation effect), so the movement index n has been the focus in the theoretical study of vortex flow field. At present, most researches on the flow field of cyclone separation are used water as medium and based on Newton flow field, most scholars' researches [3] show that the index of combination vortex motion is a constant and its value in widely used calculation formula is 0.64. However, our group that early used water as medium found that the value of index n was not a constant but a value varying from 0 to 1 along variation of the radius of Hydrocyclone [4].

With the development of cyclone technology and oilfield development technology, media become more complicated and

* Corresponding author. School of Mechanical Engineering, Southwest Petroleum University, Chengdu 610500, China.
E-mail addresses: tianjialin001@gmail.com, 309009838@qq.com (J.-L. Tian).
Peer review under responsibility of Southwest Petroleum University.

Production and Hosting by Elsevier on behalf of KeAi

http://dx.doi.org/10.1016/j.petlm.2015.05.001

most of separation media are typical non-Newtonian fluid with big apparent viscosity. Non-Newtonian rheology makes separation effect reduced obviously or even lose efficacy, which has attracted some scholars' attentions. In their studies, Dyakowski [5,6] and Tavares [7] carried out the numerical simulation about the flow of power-law fluid in the 50.8-inches diameter cyclone, which shown that the rheological property had an effect on magnitude of tangential velocity near the axis. Kawatra [8] and Walker [9] used the experiment to study the effect of mud viscosity on separation efficiency. In the domestic, Liu Xiaoming [10], Cai Pu [11] and others also are working on the non-Newtonian vortex flow fields, but on the whole, the existing researches are not many, and the results are only limited to qualitative researches and stay at the level of general distribution rule and influence trend. The quantitative mathematical descriptions between non-Newtonian rheology and key parameters of flow field have not been reported.

Because of the complexity of the vortex flow field and turbulent flow theory's development restriction, its mathematical model is very difficult to be directly described and the images of imaging technology of experimental method for non-Newtonian flow field is also hard to be directly used for quantitative analysis, so using CFD (numerical simulation method) for quantitative researches of non-Newtonian flow field with the changes of apparent viscosity of shear rate is very applicable. This paper uses the mature and reliable CFD and model [12] and is based on the existing research results in Newton flow field. Comparing with the simulation experiment data of Newton flow field (water), the influence mechanisms of the cyclone flow field key parameters were quantificationally analyzed by non-Newtonian rheology of different media.

2. Analysis model

2.1. Model grid and acquisition point

In order to facilitate comparative studies, the cyclone model that this paper selects is determined according to the proportion of literature [2] model, the specific parameters are as follows: the nominal diameter is 75 mm, length of cylindrical section is 75 mm, liquid inlet diameter 25 mm, diameter of overflow hole is 25 mm, insertion depth of overflow pipe is 50 mm, diameter of underflow port is12.5 mm. Fig. 1 is the three-dimensional model's whole calculation domain (generating 56,674 hexahedrons and 10,624 quadrilateral hybrid grids, a total of 1,63,743 grid nodes). The axis of cyclone is defined as Z axis, the plane where the underflow port lies is $z = 0$, the axis is defined every 10 mm upward and the direction upward along the axis of cyclone is positive. The two mutually perpendicular X and Y planes through Z axis are defined as two longitudinal sections. Since the absolute motion of internal fluid is a spiral rotating flow, not completely symmetrical, in order to quantitatively study parameter values at some specific radius r more reasonably, we define four points X+, X−, Y+, Y− of radius r, as shown in Fig. 2, read the data values at the four points, and the average value of their parameters represents the value at radius r, the data collection points are set along the radius direction every 0.5 mm.

2.2. Model selection and boundary

The cyclone's internal fluid motion is a complex three-dimensional flow, the tangential velocity gradient is large, and strong swirling turbulence makes Reynolds stress have the characteristics of anisotropy. For FLUENT's numerical calculation, the choice of a model is crucial. To study the movement characteristics, RSM is used on the basis of the turbulence model with anisotropy, the model has been believed to be the most applicable by many scholars, and the basic equation (and Mixture) can be referred to related articles [13]. What's more, the essential difference between non-Newtonian and Newtonian fluid lies in the cause that the apparent viscosity will change with the change of shear rate, so the model is more suitable for non-Newtonian cyclone separation flow field. For the calculation of non-Newtonian flow field, we only need to replace the molecular viscosity term in the equation with apparent viscosity. For several typical non-Newtonian power-law fluid that this article simulates, the related parameters of apparent viscosity of non-Newtonian power-law model fluid can be directly set in the viscosity parameters setting of non-Newtonian-power-law, and the parameters that need inputting are: K is the average viscosity coefficient (consistency coefficient) of fluid, n is the non-Newtonian strength coefficient (power-law index) of fluid, T is the reference temperature, the minimum viscosity limit and maximum viscosity limit are respectively the lower and upper limit of power-law fluid's apparent viscosity. If the apparent viscosity calculated according to the power-law fluid model exceeds the range, we will use the setting value instead of calculated viscosity value. Because the viscosity span of the simulated medium is large in this article, the maximum value should be set as big as possible. In this article, the maximum value is set as 100, and the smallest value is set as 0.0001, which ensure convergence of iterative calculation. The apparent viscosity of power-law model [14] is:

$$\eta = K \cdot \gamma^{n-1} \tag{1}$$

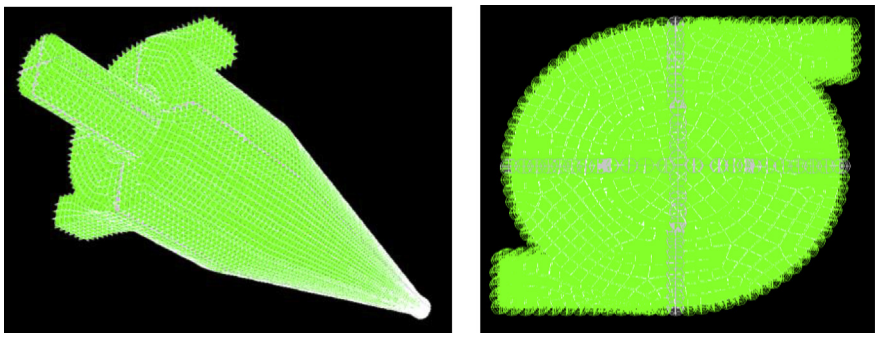

Fig. 1. Simulation test with the cyclone grid structure.

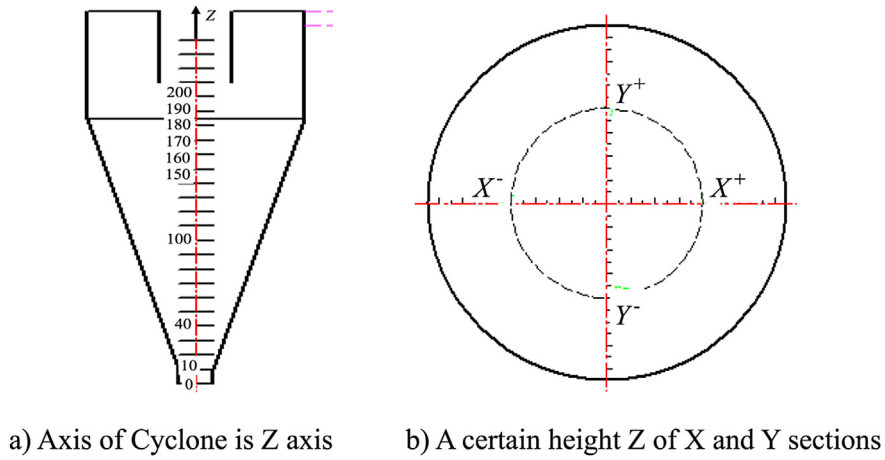

Fig. 2. Cyclone schematic diagram of the internal flow field position calibration.

where η is apparent viscosity, Pa·s, K is consistency coefficient, or power-law coefficient, Pa·s, n is non-Newtonian index or power-law index.

In order to get the comparative study's results between Newton and non-Newtonian motions in the cyclone separation flow field, we select several typical non-Newtonian fluids with power-law models to illustrate the effect of different rheological characteristics on the cyclone separation flow field. The fluids are the most applied separation media in the field job of cyclone separation, which are respectively sewage flooding, crude oil and drilling fluid polymers. At the same time, in order to guarantee the fluid can form the double helix structure of centrifugal force field after entering the cyclone. The boundary conditions of this paper are set: the entrance velocity for the drilling fluid's optimal operation parameters is 20 m/s, the ratio of dominant term is 100%, the ratio of gas volume is 0.001. The export is set to directly communicate with atmosphere, air return coefficient is 1. Set the cyclone walls are all stationary “no slip” WALL. The four different kinds of physical parameters of viscosity media are in Table 1.

3. Simulation results and analysis

When the cyclone is in the normal work, its internal flow field is a combination vortex flow field with the intermediate for forced vortex and the periphery for (quasi) free vortex. Without considering the liquid viscous resistance, the distribution law of tangential velocity along the radius is [15]:

$$v_t r^n = v_{kt} R^n = C \tag{2}$$

where R and r are respectively the nominal radius of cyclone and the rotational radius of fluid in the cyclone, v_t is the tangential velocity of fluid at the radius r of the cyclone, v_{kt} is the tangential velocity of fluid at the cyclone wall (at the maximum radius), n is the structural parameters (free vortex motion index), C is a constant.

From the formula, to determine the index n value of combination vortex motion, it can be obtained by the tangential velocity of the flow field and the radius of cyclone, and the simulation analysis can just read the simulation experiment data of tangential speed at the radius r of data acquisition point.

Table 1
Parameter Settings of the comparative study between Newton and non-Newtonian fluid.

Type	Inlet velocity (m/s)	Density (kg/m3)	Consistency coefficient K(Pa sn)	Flow index N
Water	20	998.2	0.00103	1
Polymer flooding sewage	20	998.2	0.0418	0.7223
Drilling fluid	20	1490	0.135	0.85
Crude oil	20	947.4	2.5042	0.9573

3.1. Simulation results

From the comparison figure of the distribution law in Fig. 3, non-Newton fluid and Newton fluids in the distribution of tangential velocity are similar, while we can see clearly from the cloud chart that the maximum tangential velocity surface at the 3/2 area near the overflow port. Fig. 3 a) and b) display that the spiral motion of fluid appears obvious asymmetry when the entrance velocity is 20 m/s, while the symmetry of drilling fluid in Fig. 3 c) is very good, which can explain that the separation media with different viscosities exist an entrance average speed of optimal operation, namely the problem of the handing capacity commonly used in the project. For the heavy oil in Fig. 3 d), its tangential velocity comes to the maximum near the entrance. The tangential velocity drops very quickly among the following whole flow and the more down, the lower the speed value is, which can explain that the heavy oil moves slowly under the entrance velocity 20 m/s because of its high apparent viscosity, simply can't develop into a turbulent state and form a spiral motion.

In Fig. 4, the distributions of turbulent viscosity of media a) b) and c) have similarities: the turbulent viscosity increases gradually from the boundary layer along the direction of radius inwards in the main separation zone. Due to the effect of medium viscosity, the turbulent viscosity of boundary layer is small. With the increase of tangential velocity, fluid starts to do the strong rotation motion. For its velocity gradient is large, the strong eddy diffusion and cascaded hash start to increase by random fluctuation between the layers of fluids, the exchange between various physical quantities increases, and the turbulent viscosity also increases. Because of low viscosity, Newton fluid water a) develops into a fully turbulent state quickly near the entrance, so the turbulent viscosity will increase quickly, while the polymer flooding wastewater b) and drilling fluid c), because of the apparent viscosity, will appear to have higher values of turbulence viscosity in the main separation zone. The maximum value of heavy oil appears at the entrance, this is due

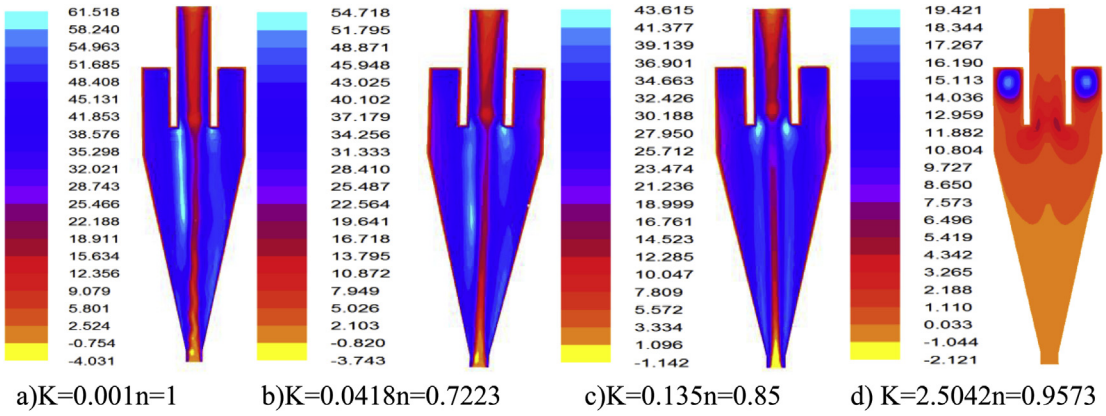

Fig. 3. Contrast cloud chart of the distribution of different media's tangential velocity.

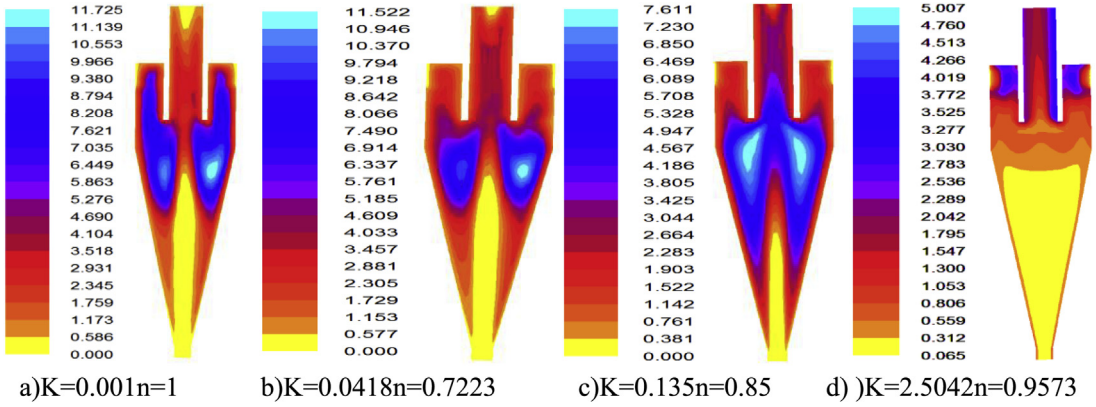

Fig. 4. Contrast cloud chart of the distribution of turbulent viscosity.

to its large apparent viscosity. After entering the cyclone, the heavy oil forms a vortex at the entrance due to the viscosity effect itself, while the subsequent flow field is hard to develop into turbulence and can't form a combination vortex motion.

3.2. Simulation data

By quantitative contrast analysis, the average value at the data acquisition point is read. For the crude oil can't form a combination vortex motion under the above conditions, its combination vortex index is no longer analyzed. In Fig. 5, the circle, triangle and cross curves represent the distribution curves of tangential velocity of water, polymer flooding wastewater and drilling fluid respectively. Under the same feed speed conditions, with the increase of medium apparent viscosity, the non-Newton and Newton flow field is still a combination vortex flow field with the interior for forced vortex and the periphery for quasi free vortex. As is known, apparent viscosity is an important parameter in the vortex flow field and the apparent viscosity of non-Newtonian fluid is larger than water. From a quantitative point of view in Fig. 5, in the same radius, the water has minimum apparent viscosity, but it has largest tangential velocity. Conversely, drilling fluid has largest apparent viscosity, but it has minimum tangential velocity. In summary, the paper believes that the most fundamental reason of the tangential velocity decrease is that the apparent viscosity of non-Newtonian fluid is larger than water, which is also proved by the research results of Dyakowski [4,8]. Furthermore, with the increase of the radius, the tangential velocity reaches at the peak point and then decreases. At the peak point, the velocity values decreases from the water' (μ = 1 mPa s) 54.153 m/s to the polymer flooding wastewater' 47.737 m/s, and then decreases to the drilling fluid' 37.527 m/s; The radius corresponding to the maximum tangential velocity is also different, indicating that the maximum tangential velocity surface, the gas–liquid's exchange interface of forced vortex and quasi free vortex, and the sizes of air column are all different.

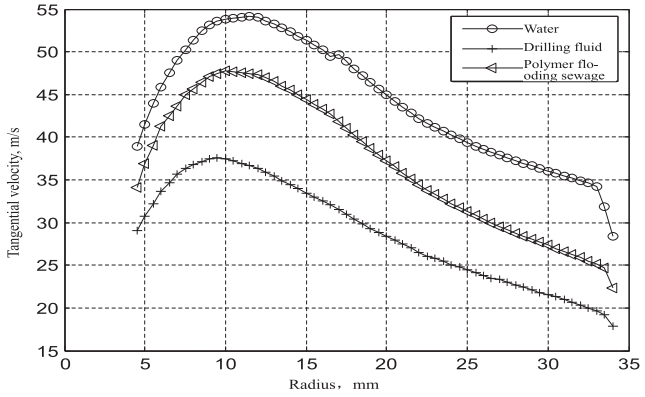

Fig. 5. Tangential velocity of Newton fluid and non-Newtonian fluid.

Table 2
Calculation of constant section of combination vortex motion index n.

Media Type	Water	Polymer flooding sewage	Drilling fluid
Vortex index n	0.564	0.769	0.699

3.3. The calculation results for the value of index n of combination vortex motion

Putting all of the above points' tangential velocity data and the simulation cyclone's specific parameters (R = 37.5 mm, v_{kt} = 20 m/s) into the formula (2), the calculation result (drawn in Fig. 5) of Table 3 is obtained by the iteration every 0.5 mm in the combination vortex motion region. Fig. 6 shows clearly the comparison graph of the value of combination vortex index n of water (circle), drilling liquid (cross) and polymer flooding wastewater (triangle) under the same conditions, it can be seen that the distribution rules of the three media with different rheology have similarities in the flow field of different combination vortex motion regions. At the outermost end of the combination vortex motion, namely r = 34 mm <0.5 (R-Δ) times of the radius (r = 17), also namely the outside-quasi free vortex area, the combination vortex indexes of non-Newton and Newton fluids along the radius direction can be approximately seen as a constant. At about the 0.5 R times of the radius (r = 17)–r = 5 mm region, namely the outside-quasi free vortex area translating to forced vortex area, both of the combination vortex motion index n are approximately in a linear distribution of certain gradient. From the numerical analysis, the three media's combination vortex motion indexes have certain differences, in the region of r > 17 mm, through the average calculation, the values of constants n of the three combination vortex are: 0.564(water), n = 0.769, drilling fluid 0.708 (polymer flooding wastewater), and the range ability of non-Newton fluid in the average value's region is larger than that of Newton fluid, which should be the result that the shear thinning apparent viscosity of non-Newton power-law fluid with shear thinning type is changing in the average value's region, but can be seen as change along a constant value. While in the r < 17 mm region, the three can be approximately seen as three parallel oblique lines whose expression of slope can be seen as the same.

3.4. Phenomenon of turbulent drag reduction

It argues that the value of movement index n of water's free vortex area is less than those of the two kinds of non-Newtonian fluids, which is caused by the characteristics of turbulent drag reduction of non-Newtonian fluid. Many scholars researched the phenomenon of turbulent drag reduction. Tom B A [16] thought turbulent drag reduction effect of non-Newtonian fluid and its application were to add high molecular polymer solvent to clear water and make it to be shear thinning non-Newtonian fluid, and then raised its head of delivery at a certain rate of turbulent flow field; Toms and Krame successively found polymer dilute solution or elastic protective material could achieve viscosity drag reduction. Other articles [17,18] studied the mechanism of turbulent drag reduction, water due to minimum molecular viscosity, should have the highest degree of freedom, namely the combination vortex motion index should be the biggest, but due to the minimum molecular viscosity, it led to high turbulence and fast kinematic velocity when entering the cyclone. In the process, the friction between the molecules intensified and high turbulent viscosity led to serious internal loss. From Fig. 4, it can clearly reflect the phenomenon of turbulent drag reduction, but for the polymer flooding sewage, the turbulent viscosity in the same area is less than water and the freedom degree of fluid is greater than water instead. At the same time its value of consistency coefficient K and flow index are less than drilling fluid, resulting in smaller apparent viscosity. Furthermore, the shear thinning character is stronger than drilling fluid, the apparent viscosity will decrease faster in the area, so the polymer flooding sewage's freedom degree in the area is stronger than drilling fluid. Table 2.

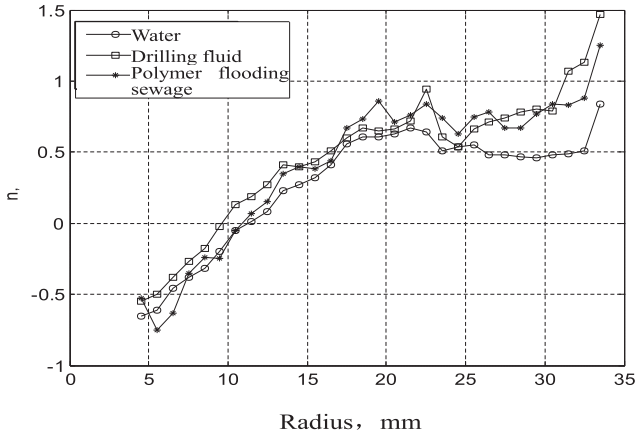

Fig. 6. Contrast of combination vortex index n between Newton fluid (water) and non-Newtonian fluid (drilling fluid and polymer flooding sewage).

4. Quantitative expression and verification of index n

In summary, the segmented function of the value of combination vortex motion index n considering the non-Newtonian rheology is presented:

Table 3
Calculation results of combined vortex motion index n in main separation region.

r	4.5	5	5.5	6	6.5	7	7.5	8	8.5	9	9.5
n	−0.544	−0.518	−0.487	−0.467	−0.369	−0.351	−0.246	−0.169	−0.164	−0.144	−0.006
r	10	10.5	11	11.5	12	12.5	13	13.5	14	14.5	15
n	0.046	0.164	0.209	0.219	0.229	0.309	0.421	0.437	0.454	0.467	0.477
r	15.5	16	16.5	17	17.5	18	18.5	19	19.5	20	20.5
n	0.496	0.514	0.606	0.722	0.763	0.802	0.843	0.864	0.825	0.793	0.824
r	21	21.5	22	22.5	23	23.5	24	24.5	25	25.5	26
n	0.855	0.888	0.889	0.837	0.747	0.694	0.711	0.730	0.729	0.721	0.695
r	26.5	27	27.5	28	28.5	29	29.5	30	30.5	31	31.5
n	0.686	0.690	0.703	0.705	0.709	0.729	0.757	0.778	0.801	0.832	0.876
r	32	32.5	33	33.5	34	34.5	35				
n	0.928	0.963	0.994	1.297	4.983	8.294	14.841				

Table 4
Contrast of different formulas for tangential velocity.

Proposer	Different formulas in main separation region
Pang Xueshi [19]	$v_t = 3.7\frac{r_i'}{R}v_i\left(\frac{R}{r}\right)^{0.64} \quad (i = 0, 1, 2...)$
Previous research	$v_t = v_i\left(\frac{R}{r}\right)^{\frac{4r}{R+3r}} \quad (2r_0/3 < r < R)$
Present research	$v_{t_{i+1}} = v_{t_i}\left(\frac{r_i}{r_{i+1}}\right)^{n_{(i+1)}} \quad (i = 0, 1, 2...)$

$$n = \begin{cases} \dfrac{n_f r}{0.5(R-\Delta)} - 1 & 0 < r \le 0.5(R-\Delta) \\ n_f & 0.5(R-\Delta) < r \le \Delta \end{cases} \tag{3}$$

where n is the combination vortex motion index, n_f is the constant period average of combination vortex movement index corresponding to non-Newtonian fluid, R is the engineering radius of cyclone, mm, r is the corresponding radius, mm, Δ is the thickness of boundary layer, mm, which is 0.1 R under the working condition.

In order to verify the correctness of analysis results in this paper, we put the above calculation result and specific parameters of simulation cyclone (R = 37.5 mm, v_i = 20 m/s) into the formula (2), and can reversely get the corresponding tangent velocity values of all radii. Compared with the combination vortex index n (0.64) of the cyclone's universal-design calculation formulas, the numerical simulation results have great difference. The result value in various regions of the original formula is greater than that in the actual flow field of tangential velocity, because the formula is based on the empirical formula of ideal fluid theory, not considering the influence of medium and turbulent viscosity, more not considering the influence of non-Newtonian rheology. The calculation result of this paper, not only in trends but the values has well coincide with the simulation values, the error is very small within 5%, it should be because of simplifying combination vortex index n in the region. So the calculation method this paper puts forward and the influence of non-Newtonian medium's rheology considered are more coincide with the actual situation of real flow field, which can be the basis of calculation theory of non-Newtonian medium's velocity field. Table 4 Figs. 7 and 8.

In the formulas, v_i is the average feeding speed, m/s; v_t is the tangential velocity at radius r, m/s; r_i' is the radius of liquid inlet pipe, mm; r_i and r_{i+1} are the radii of the adjacent points respectively; v_{ti} is the tangential velocity at radius r_i, m/s; $n_{(i+1)}$ is the combination vortex index at the radius r_i (see Fig. 9).

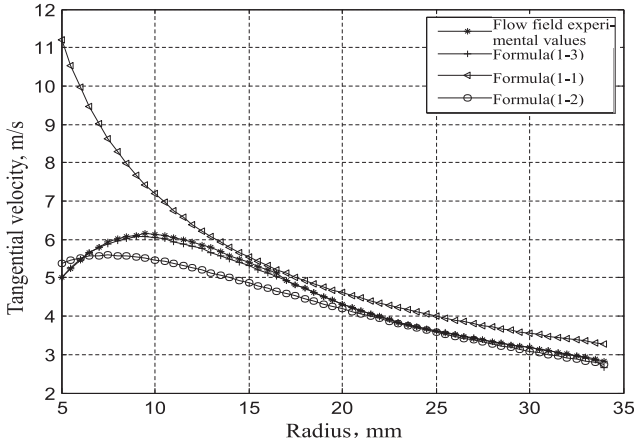

Fig. 7. Tangential velocity contrast between different calculation formulas and drilling fluid (1-3).

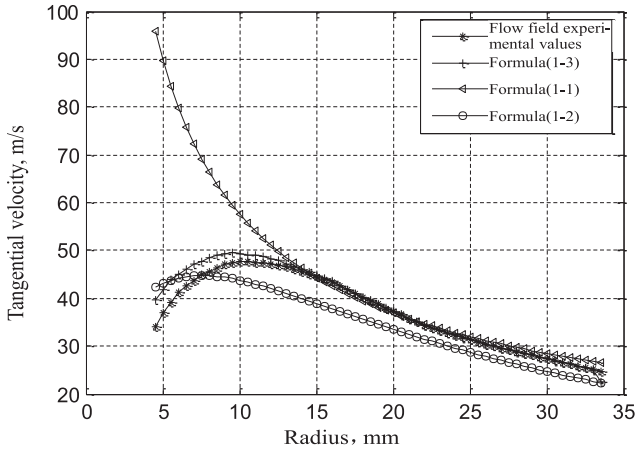

Fig. 8. Tangential velocity contrast between different calculation formulas and polymer flooding sewage (1-3).

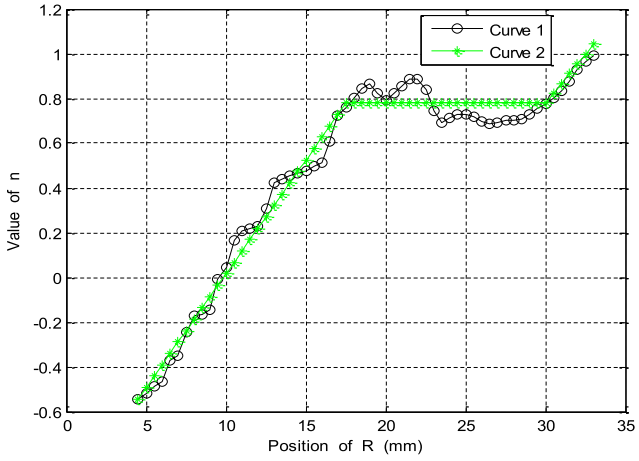

Fig. 9. Contrast curve of n value of initial calculation and formula calculation.

5. Conclusions

By applying FLUENT and combining the power-law model with RSM and Mixture. The 3D numerical simulation is carried out to combination vortex motion of non-Newtonian flow field in the cyclone. The results show that non-Newtonian rheology has a great influence on tangential velocity that decreases with the increase of non-Newtonian rheology, namely turbulent drag reduction. Compared with Newton flow field, the tangential velocity and combination vortex motion index of non-Newtonian flow field is analyzed quantitatively, and the corresponding calculation formulas are given. The results show that the quantitative description in this paper fully reflects the effect of non-Newtonian rheology on the cyclone separation flow field and as the theoretical basis of flow field, more accurately matches the actual flow field than Newton (water).

References

[1] Liu Yaojun, Prospects for the application of cyclone separator in oil field engineering, Acta Pet. Sin. 19 (3) (1998) 110–115.

[2] K.T. Hsieh, R.K. Rajamani, Mathematical model of the hydrocyclone based on physics of fluid flow, AIChE J. 37 (5) (1991) 735–746.
[3] Liang Zheng, Ren Liancheng, Zhong Gongxiang, Wu Shihui, The hydrocyclone structure parameters n of quantitative research, Coal Mine Mach. 27 (10) (2006) 53–56.
[4] T. Dyakowski, R.A. Williams, Prediction of high solids concentration regions within a hydrocyclone, Powder Technol. 87 (1996) 43–47.
[5] L.M. Tavares, L.L.G. Souza, J.R.B. Lima, M.V. Possa, Modeling classification in small-diameter hydrocyclone under variable rheological conditions, Min. Eng. 15 (2002) 613–622.
[6] S.K. Kawatra, A.K. Bakshi, M.T. Rusesky, The effect of slurry viscosity on hydrocyclone, Min. Process 48 (1996) 39–50.
[7] K.J. Walker, T.J. Veasey, I.P.T. Moore, A parametric evaluation of the hydrocyclone separation of drilling mud from drilled rock chippings, Chem. Eng. 71 (1993) 312–313.
[8] T. Dyakowski, G. Hornung, R.A. Williams, Simulation of non-Newtonian flow in a hydrocyclone, Chem. Eng. 72 (1994) 513–520.
[9] Min Zhang, Lvhong Zhang, et al., Non-Newtonian fluid mixing flow field numerical simulation research progress, J. Chem. Ind. Rev. 28 (8) (2009) 1296–1301.
[10] Xiaoming Liu, ZhiJiu Yi, et al., Non-Newtonian fluid and Newtonian fluid flow field in the cyclone analysis, J. Pet. Mach. 37 (3) (2009) 28–31.
[11] Pu Cai, Wang, Inside the hydrocyclone non-Newtonian fluid multiphase flow field numerical simulation, J. Chem. Ind. 63 (11) (2012) 60–69.
[12] Liang Zheng, et al., The theory of hydrocyclone flow field numerical simulation in the choice of turbulence model, J. Nat. Gas. Ind. 27 (3) (2007) 119–121.
[13] Lin Yang, Liang Zheng, Jialin Tian, Double internal cone type oil-water separation hydrocyclone flow field numerical simulation, J. Fluid Mach. 36 (5) (2008) 30–34.
[14] Li Zhaomin, Non-Newtonian Fluid Mechanics, Higher Education Press, 1998, p. 4.
[15] Pang Xueshi, Basic properties of spiral vortex and its role in the cyclone, J. Non Fer. Met. (4) (1991) 30–34.
[16] B.A. Tom, Congress on Rheology, Academic Press, North Holland, 1948, p. 135.
[17] Bingjiang Zhang, Guangchuan Liang, The turbulent drag reduction mechanism of polymers, J. Oil Gas. Storage Transp. 31 (12) (2012) 95–98.
[18] James B. Crews, Tianping Huang, Internal Breakers Forviscoelastic-Surfactant Fracturing Fluids, SPE106216, 2007.
[19] Pang Xueshi, The basic properties and the role of spiral vortex in the cyclone, Non Ferr. Met. (4) (1991) 30–34.